Otology & Neurotology
31:256–266 © 2010, Otology & Neurotology, Inc.

Deregulated Genes in Sporadic Vestibular Schwannomas

*†Per Cayé-Thomasen, ‡Rehannah Borup, *†Sven-Eric Stangerup, *†Jens Thomsen, and †‡Finn Cilius Nielsen

**The Department of Oto-rhino-laryngology, Head and Neck Surgery, Gentofte University Hospital; †The Faculty of Health Sciences, University of Copenhagen; and ‡The Department of Clinical Biochemistry, Copenhagen University Hospital, Copenhagen, Denmark*

Objective: In search of genes associated with vestibular schwannoma tumorigenesis, this study examines the gene expression in human vestibular nerve versus vestibular schwannoma tissue samples using microarray technology.
Material and Methods: RNA was extracted from 3 vestibular nerves (serving as control) and 16 solid, sporadic vestibular schwannomas. RNA (5 μg) was used in the labeling and biotinylation protocol to produce cRNA, which was hybridized to Affymetrix HG-U133A arrays. Data were imported into dChip v.1.3 and normalized using invariant set normalization. Differentially expressed genes were identified as differences between control and tumor tissue larger than 2-fold, with a conservative *p* value of less than 0.000001 and means of differences greater than 25.
Results: Eighty-seven probe sets, representing 78 genes, were significantly up- or down-regulated in tumor tissue. The deregulated genes were matched against established gene ontology, revealing that 8 of the up-regulated genes are involved in regulation of the cell cycle, 6 in cell morphogenesis, 8 in cell development, 11 in cell differentiation, 6 in cell death, 13 in cell adhesion, 9 in extracellular matrix, and 50 in protein binding (overlapping occurring). Gene annotation enrichment analyses of the clustered genes showed significant enrichment of annotations for the extracellular matrix ($p < 0.0002$), cell adhesion ($p < 0.0001$), and protein binding ($p < 0.0004$).
Conclusion: We conclude that a number of transcripts are deregulated in sporadic vestibular schwannomas, and that several of these have functional annotations implicated in tumorigenesis. Specifically, genes involved in extracellular matrix function, cell adhesion, and protein binding seem to be of potential importance. However, further studies using other methodologies are needed for verification of the observed changes of gene expression seen by cDNA microarray analyses, for example, reverse-transcriptase–polymerase chain reaction and protein analyses. **Key Words:** Acoustic neuroma—cDNA microarray—Gene expression—Tumorigenesis—Vestibular nerve.
Otol Neurotol **31:**256–266, 2010.

The occurrence of both sporadic and NF2-associated vestibular schwannomas is associated with a loss of or a mutation in a tumor suppressor gene on chromosome 22q12 (1,2). The gene encodes the protein merlin or schwannomin, which normally accumulate under specialized regions of the cell membrane and functions as a membrane organizer and a linker of the cytoskeleton (3). Merlins tumor suppressor function is likely to be linked to regulation of actin cytoskeleton-mediated processes and cell proliferation (reviewed in 4,5).

Address correspondence and reprint requests to Per Cayé-Thomasen, M.D., D.M.Sc., Department of Oto-rhino-laryngology, Head and Neck Surgery, Gentofte University Hospital of Copenhagen, DK-2900 Hellerup, Denmark; E-mail: peca@geh.regionh.dk

Financial support was granted from Hans Skouby's og hustru Emma Skouby's Foundation and The Faculty of Health Sciences, University of Copenhagen, Denmark.

However, not all vestibular schwannomas exhibit inactivation of the merlin/schwannomin (4,5), and the phenotypical characteristics of those that do demonstrate a high degree of variability. Tumor growth rate and cyst formation are 2 clinically very important examples of variables concerning the phenotype.

In search of genes and pathways associated with vestibular schwannoma tumorigenesis, Welling et al. (6) used cDNA microarray analysis of tissue samples from 1 vestibular nerve versus 3 cystic sporadic, 3 solid sporadic, and 1 NF2-associated vestibular schwannoma. The human transcriptome was screened and a number of deregulated genes identified in tumor tissue, for example, upregulation of the angiogenesis mediators endoglin and osteonectin (SPARC), downregulation of the apoptosis-related LUCA-15, and deregulation of the protein 4.1 superfamily members ezrin, radixin, and moesin, which are very similar to merlin. However, the limited number

FIG. 1. "Heat-map" of the clustered genes. Of the 78 deregulated genes in vestibular schwannoma tumor tissue, 3 were downregulated (shown at the *top*) and 75 upregulated (*below*). The color intensities of the heat-map indicate the degree of deregulation (*blue* indicates relative downregulation and *red* relative upregulation). A *vertical line of colored squares* represents 1 tissue sample. The 3 controls (adjacent vestibular nerve) are shown to the *right*, the 16 tumors to the *left*.

of samples in this pioneering study was a disadvantage, which precluded meaningful statistical analyses.

The present study examines the gene expression in tissue samples from 3 human vestibular nerves versus 16 solid, sporadic vestibular schwannomas using a microarray chip that quantitates the tissue content of individual mRNA molecules transcribed from the entire human genome, covering more than 20,000 genes. The aims were to identify deregulated genes and functional areas of potential importance for tumorigenesis to generate hypotheses and pinpoint potential areas of future research.

MATERIAL AND METHODS

Patient Data

Noncystic, solid, unilateral vestibular schwannoma tissue was sampled prospectively from 16 patients after translabyrinthine tumor excision. In 3 of the 16 cases, the tumor was excised en bloc with an intact and microscopically normal piece of the vestibulocochlear nerve attached, representing the part of the nerve located between the tumor and the brainstem. The microscopically normal piece of nerve was dissected meticulously from the tumor (to avoid contamination by tumor cells) and served as "normal" control. Tumor sample and vestibular nerve tissue were snap-frozen immediately after tumor removal and stored at −80°C. Conventional microscopy of the remaining part of the tumor confirmed the diagnosis.

Debut symptom was hearing loss and/or tinnitus in all cases. The mean age at operation was 51.4 years (range, 26–65 yr; standard deviation, 8.7). The male-to-female ratio was 1.67. Mean largest extrameatal tumor diameter at the last preoperative magnetic resonance scan was 17.9 mm (range, 13–25 mm; standard deviation, 3.0).

Microarray Analysis

Total RNA was extracted using Trizol according to standard procedures. RNA (5 μg) was used to synthesize double-stranded cDNA using Superscript Choice System (Invitrogen, Carlsbad, CA, USA) with an oligo-dT primer containing a T7 RNA polymerase promoter (GenSet). The cDNA was used as a template for in vitro transcription reaction to synthesize biotin-labeled antisense cRNA (BioArray high-yield RNA transcript labeling kit; Enzo Diagnostics, Farmingdale, NY, USA). After incubation at 94°C for 35 minutes in fragmentation buffer (40 mM Tris, 30 mM MgOAc, 10 mM KOAc), the labeled cRNA was hybridized for 16 hours to HG-U133A arrays (Affymetrix Inc., Santa Clara, CA, USA). The arrays were washed and stained with phycoerytrin conjugated streptavidin (SAPE) using the Affymetrix Fluidics Station 400 before the arrays were scanned in the Affymetrix GeneArray 2500 scanner, as described in the Affymetrix GeneChip protocol.

Microarray Data Analysis

The image files (cell files) were imported into the software package DNA-Chip Analyser (C. Li and W.H. Wong; http://www.dchip.org) (7). The array files were normalized using the multiarray invariant-set normalization method. The normalization was based on probes that have similar rank in the baseline and experiment array (invariant set). The invariant set was used to generate a piecewise linear median curve between the baseline probes and the experiment probes, which is used as the normalization curve (7). Model-based expression indices were calculated using the PM/MM model implemented in dChip version 1.3.

Hierarchical clustering was done according to the algorithm in dChip version 1.3, with a distance measure of 1 minus the Pearson correlation coefficient applying the average linkage algorithm, with a p value threshold of 0.001 for significant sample clusters.

Differentially expressed genes were identified as differences between control and tumor tissue larger than 2-fold, with a conservative p value less than 0.000001 and a differences of means greater than 25.

The deregulated genes were matched against the established gene ontology (GO) database using the built-in annotation functionality in dChip, which is based on GO information from the Gene Ontology Consortium (8).

Gene annotation enrichment analyses of the deregulated genes were performed against established GO clusters using the hypergeometric tests to assess overrepresentation (enrichment) of Gene Ontology categories.

For the number of genes in the deregulated gene list that are assigned to a given GO function, the hypergeometric p value was calculated for overrepresentation or underrepresentation of that particular function in the total number of deregulated genes as compared with the relative representation of that GO function in all annotated genes on the array.

RESULTS

A hierachial cluster of downregulated and upregulated probes/genes in tumor tissue is shown in Figure 1, and the fold change of the individual probes/genes is displayed in Table 1.

Only 3 transcripts encoding glycoprotein M6A, ribosomal protein S6 kinase, and vitelliform macular dystrophy 2 (bestrophin 1) were significantly downregulated using the previously described criteria.

Eighty-four probes were upregulated, corresponding to 75 different transcripts (Table 1).

All deregulated transcripts were matched against established GO (8), which revealed that 8 of the upregulated genes are involved in regulation of the cell cycle (Fig. 2), 6 in cell morphogenesis (Fig. 3), 8 in cell development (Fig. 4), 11 in cell differentiation (Fig. 5), 6 in cell death (Fig. 6), 13 in cell adhesion (Fig. 7), 9 in extracellular matrix (Fig. 8), and 50 in protein binding (not displayed; overlapping occurring).

Gene annotation enrichment analyses of the clustered genes showed significant enrichment of annotations for the extracellular matrix ($p < 0.0002$), cell adhesion ($p < 0.0001$), and protein binding ($p < 0.0004$).

DISCUSSION AND CONCLUSION

Given the gene deregulation criteria of a 2-fold increase or decrease and a very conservative p value, we have identified 78 genes that were either upregulated or downregulated in vestibular schwannomas using adjacent vestibular nerve as control. The criteria were

TABLE 1. *Deregulated genes in vestibular schwannomas*

Probe set	Gene	Fold
209469_at	Glycoprotein M6A	−11.03
207671_s_at	Vitelliform dystrophy 2 (best disease, bestrophin)	−3.17
204906_at	Ribosomal protein S6 kinase, 90 kDA, polypeptide 2	−3.07
220495_s_at	Chromosome 5 open reading frame 14	2.07
200805_at	Lectin, mannose-binding 2	2.11
202441_at	SPFH domain family, member 1	2.11
212459_x_at	Succinate-CoA ligase, GDP-forming, β subunit	2.20
202006_at	Protein tyrosine phosphatase, nonreceptor type 12	2.21
200634_at	Profilin 1	2.33
201762_s_at	Proteasome (prosome, macropain) activator subunit 2 (PA28 β)	2.36
220974_x_at	Sideroflexin 3/sideroflexin 3	2.40
221059_s_at	Coactosin-like 1 (*Dictyostelium*)	2.44
212922_s_at	SET and MYND domain containing 2	2.55
208782_at	Follistatin-like 1	2.67
220189_s_at	Mannosyl (α-1,3-)-glycoprotein β-1,4-*N*-acetylglucosaminyltransferase, isoenzyme B	2.68
204053_x_at	Phosphatase and tensin homolog (mutated in multiple advanced cancers 1)	2.75
213154_s_at	Bicaudal D homolog 2 (*Drosophila*)	2.77
204076_at	Ectonucleoside triphosphate diphosphohydrolase 4	2.82
203024_s_at	Chromosome 5 open reading frame 15	2.85
207541_s_at	Exosome component 10	2.94
202657_s_at	SERTA domain containing 2	3.02
202820_at	Aryl hydrocarbon receptor	3.04
200660_at	S100 calcium binding protein A11 (calgizzarin)	3.10
201670_s_at	Myristoylated alanine-rich protein kinase C substrate	3.13
221253_s_at	Thioredoxin domain containing 5/thioredoxin domain containing 5	3.18
221641_s_at	Acyl-CoA thioesterase 9	3.18
200923_at	Lectin, galactoside-binding, soluble, 3 binding protein	3.22
208944_at	Transforming growth factor–β receptor II (70/80 kDa)	3.26
208891_at	Dual-specificity phosphatase 6	3.35
209040_s_at	Proteasome (prosome, macropain) subunit, β type, 8 (large multifunctional peptidase 7)	3.35
213455_at	Hypothetical LOC283677	3.42
209781_s_at	KH domain–containing, RNA-binding, signal transduction associated 3	3.60
210427_x_at	Annexin A2	3.60
220419_s_at	Ubiquitin-specific peptidase 25	3.60
213503_x_at	Annexin A2	3.68
202963_at	Regulatory factor X, 5 (influences HLA Class II expression)	3.77
203827_at	WD40 repeat protein interacting with phosphoinositides of 49 kDa	4.06
216264_s_at	Laminin, β 2 (laminin S)	4.14
203710_at	Inositol 1,4,5-triphosphate receptor, Type 1	4.20
204214_s_at	RAB32, member RAS oncogene family	4.29
207714_s_at	Serpin peptidase inhibitor, clade H (heat shock protein 47), member 1, (collagen binding protein 1)	4.73
201954_at	Actin-related protein 2/3 complex, subunit 1B, 41 kDa	4.79
220532_s_at	LR8 protein	4.80
202403_s_at	Collagen, Type I, α 2	4.81
204306_s_at	CD151 antigen	4.81
202990_at	Phosphorylase, glycogen; liver (Hers disease, glycogen storage disease Type VI)	4.82
218223_s_at	CK2 interacting protein 1; HQ0024c protein	5.05
203222_s_at	Transducin-like enhancer of split 1 (E(sp1) homolog, *Drosophila*)	5.16
204237_at	GULP, engulfment adaptor PTB domain containing 1	5.37
209295_at	Tumor necrosis factor receptor superfamily, member 10b	5.45
213103_at	START domain containing 13	5.87
201012_at	Annexin A1	6.04
204591_at	Cell adhesion molecule with homology to L1CAM (close homolog of L1)	6.33
202404_s_at	Collagen, Type I, α 2	6.39
212775_at	Obscurin-like 1	6.46
208476_s_at	FERM domain containing 4A	6.71
201110_s_at	Thrombospondin 1	6.84
213836_s_at	WD40 repeat protein interacting with phosphoinositides of 49 kDa	6.88
208712_at	Cyclin D1	6.93
215076_s_at	Collagen, Type III, α 1 (Ehlers-Danlos syndrome Type IV, autosomal dominant)	7.00
211161_s_at	Collagen, Type III, α 1 (Ehlers-Danlos syndrome Type IV, autosomal dominant)	7.01
206857_s_at	FK506 binding protein 1B, 12.6 kDa	7.13
219250_s_at	Fibronectin leucine-rich transmembrane protein 3	7.17
1598_g_at	Growth arrest–specific 6	7.24
202796_at	Synaptopodin	8.01
217967_s_at	Chromosome 1 open reading frame 24	8.28
217966_s_at	Chromosome 1 open reading frame 24	8.31
202748_at	Guanylate binding protein 2, interferon-inducible/guanylate binding protein 2, interferon-inducible	8.57
209087_x_at	Melanoma cell adhesion molecule	8.66
219032_x_at	Opsin 3 (encephalopsin, panopsin)	8.72
209086_x_at	Melanoma cell adhesion molecule	8.77
202458_at	Protease, serine, 23	9.13
218870_at	Rho GTPase activating protein 15	9.75
210869_s_at	Melanoma cell adhesion molecule	9.95
218638_s_at	Spondin 2, extracellular matrix protein	10.74
201508_at	Insulin-like growth factor binding protein 4	11.17
204150_at	Stabilin 1	11.81
220161_s_at	Erythrocyte membrane protein band 4.1 like 4B	12.92
203636_at	Midline 1 (Opitz/BBB syndrome)	13.83
204584_at	L1 cell adhesion molecule	14.83
221729_at	Collagen, type V, alpha 2	14.84
201109_s_at	Thrombospondin 1	15.97
201939_at	Polo-like kinase 2 (*Drosophila*)	16.01
203789_s_at	Sema domain, immunoglobulin domain (Ig), short basic domain, secreted, (semaphorin) 3C	17.64
206204_at	Growth factor receptor–bound protein 14	25.22
221730_at	Collagen, type V, α 2	39.33
219304_s_at	Platelet-derived growth factor D	54.27

TABLE 1. *(Continued)*

"Fold" indicates the mean fold-change of the individual gene in tumor tissue compared with control (adjacent vestibular nerve).

chosen after initial analyses using either more or less conservative cutoff values to provide an overview of gene expression and at the same time identify a reasonable number of genes on which to focus attention for further research. Thus, the enormous data set contains information on a number of other deregulated genes or pathways potentially involved in tumorigenesis that will appear if less conservative cutoffs are used. Furthermore, deregulated transcription is not necessarily a result of significance because posttranscriptional and posttranslational processing may modulate gene expression and

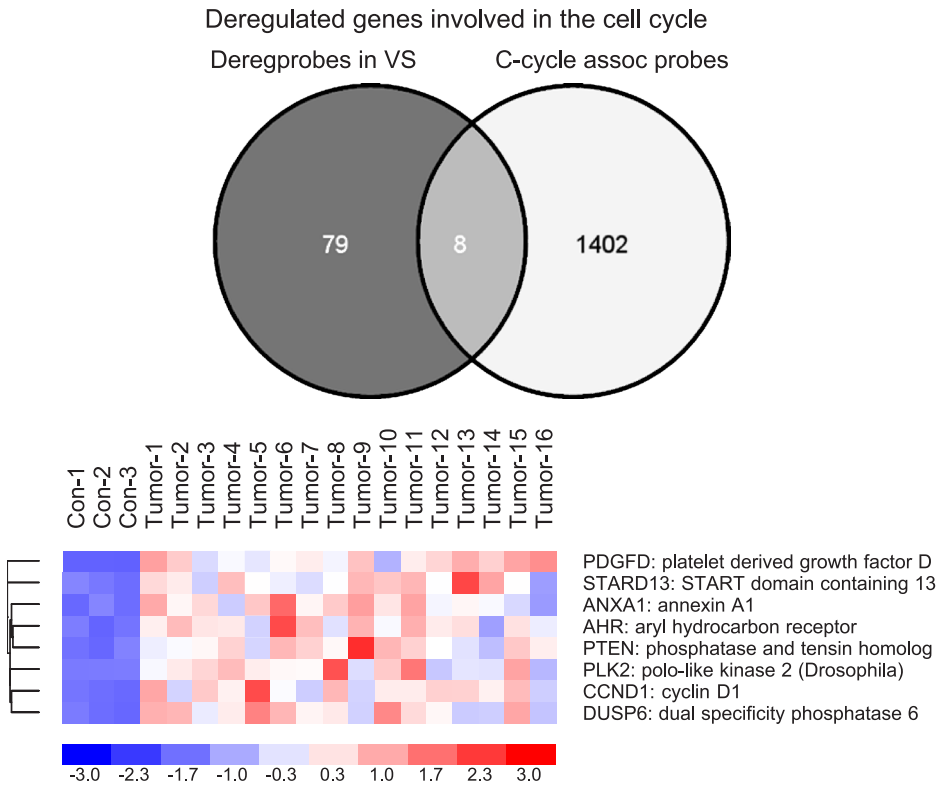

FIG. 2. Deregulated cell cycle genes. The Venn diagram display that 8 genes are common between the clustered 87 probes (78 genes) and the 1,410 probes known to be involved in the cell cycle. The 8 genes were all upregulated in tumor tissue and are listed and aligned next to the results on the "heat-map" for the 16 tumors and the 3 controls (adjacent vestibular nerves). The color intensities of the heat-map indicate the degree of deregulation, for which the standard deviation from the mean values are shown at the *bottom*.

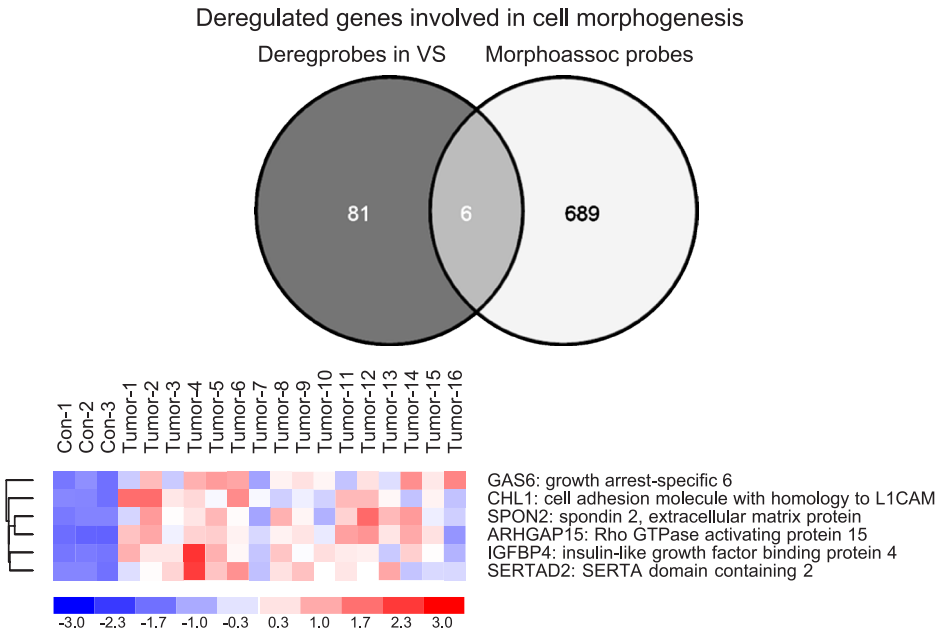

FIG. 3. Deregulated genes associated with cell morphogenesis. The Venn diagram display that 6 genes are common between the clustered 87 probes (78 genes) and the 695 probes known to be involved in cell morphogenesis. The 6 genes were all upregulated in tumor tissue and are listed and aligned next to the results on the "heat-map" for the 16 tumors and the 3 controls (adjacent vestibular nerves). The color intensities of the heat-map indicate the degree of deregulation, for which the standard deviation from the mean values are shown at the *bottom*.

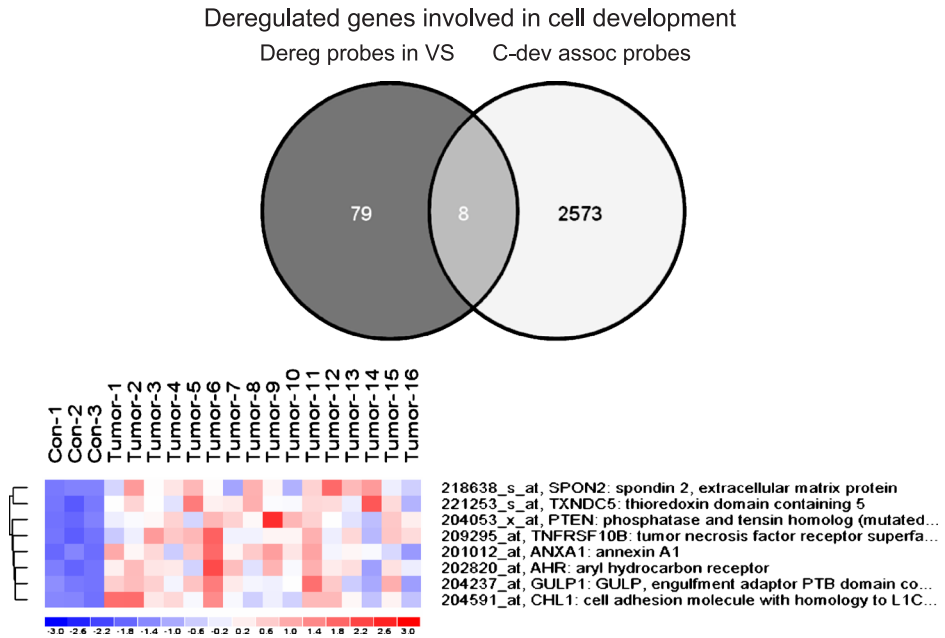

FIG. 4. Deregulated genes associated with cell development. The Venn diagram display that 8 genes are common between the clustered 87 probes (78 genes) and the 2,581 probes known to be involved in cell development. The 8 genes were all upregulated in tumor tissue and are listed and aligned next to the results on the "heat-map" for the 16 tumors and the 3 controls (adjacent vestibular nerves). The color intensities of the heat-map indicate the degree of deregulation, for which the standard deviation from the mean values are shown at the *bottom*.

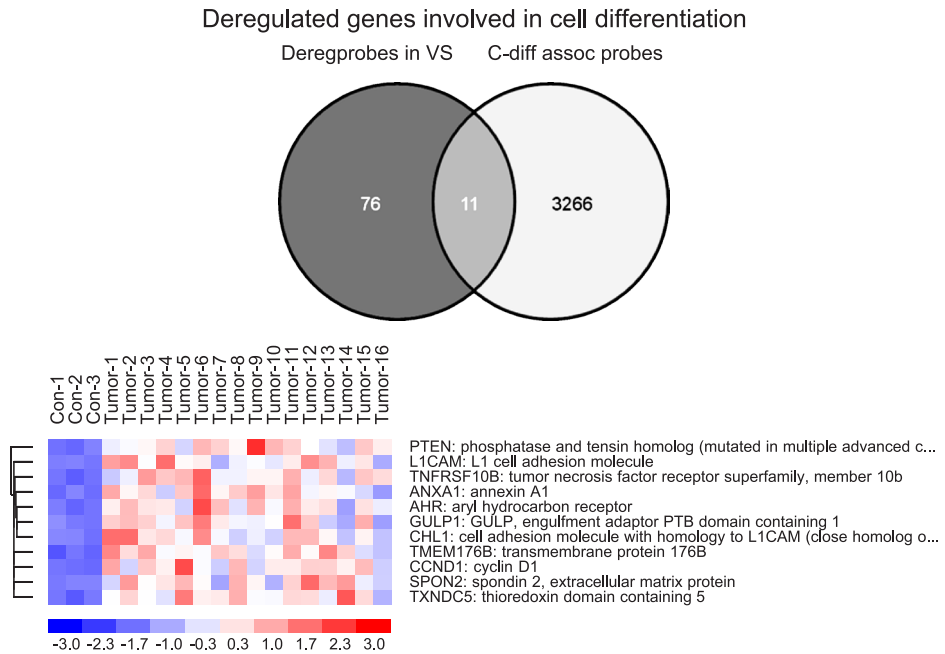

FIG. 5. Deregulated genes associated with cell differentiation. The Venn diagram display that 11 genes are common between the clustered 87 probes (78 genes) and the 3,277 probes known to be involved in cell differentiation. The 11 genes were all upregulated in tumor tissue and are listed and aligned next to the results on the "heat-map" for the 16 tumors and the 3 controls (adjacent vestibular nerves). The color intensities of the heat-map indicate the degree of deregulation, for which the standard deviation from the mean values are shown at the *bottom*.

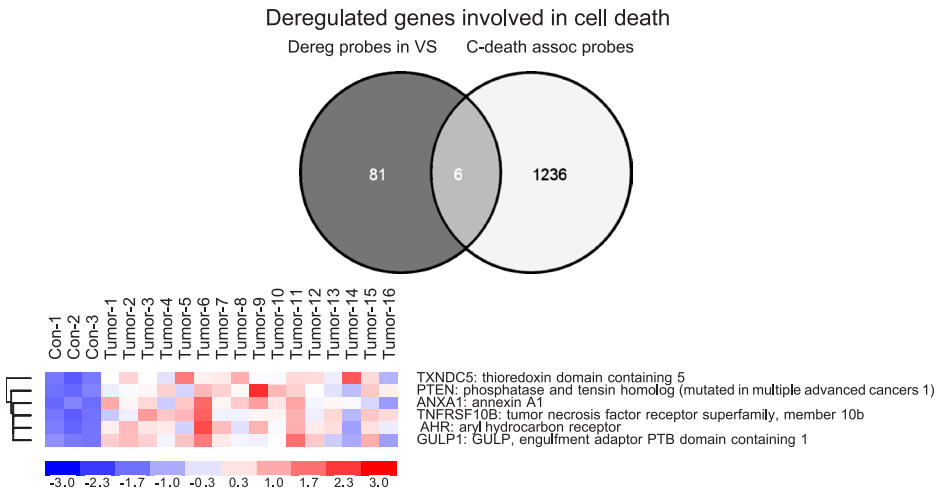

FIG. 6. Deregulated genes associated with cell death (including apoptosis). The Venn diagram display that 6 genes are common between the clustered 87 probes (78 genes) and the 1,242 probes known to be involved in cell death (including apoptosis). The 6 genes were all upregulated in tumor tissue and are listed and aligned next to the results on the "heat-map" for the 16 tumors and the 3 controls (adjacent vestibular nerves). The color intensities of the heat-map indicate the degree of deregulation, for which the standard deviation from the mean values are shown at the *bottom*.

protein function in ways of biologic importance to tumorigenesis. Furthermore, some genes may be at play in some tumors, but not in others, lending relevance to an analysis of gene expression in relation to tumor phenotype. Finally, although previous studies using the presently used microarray platform has shown a high degree of validity when comparing results to reverse-transcriptase–polymerase chain reaction (RT-PCR), the present findings have not been verified with either RT-PCR or protein expression analyses.

These precautions in mind, however, it is likely that upregulated transcripts are significant for the development

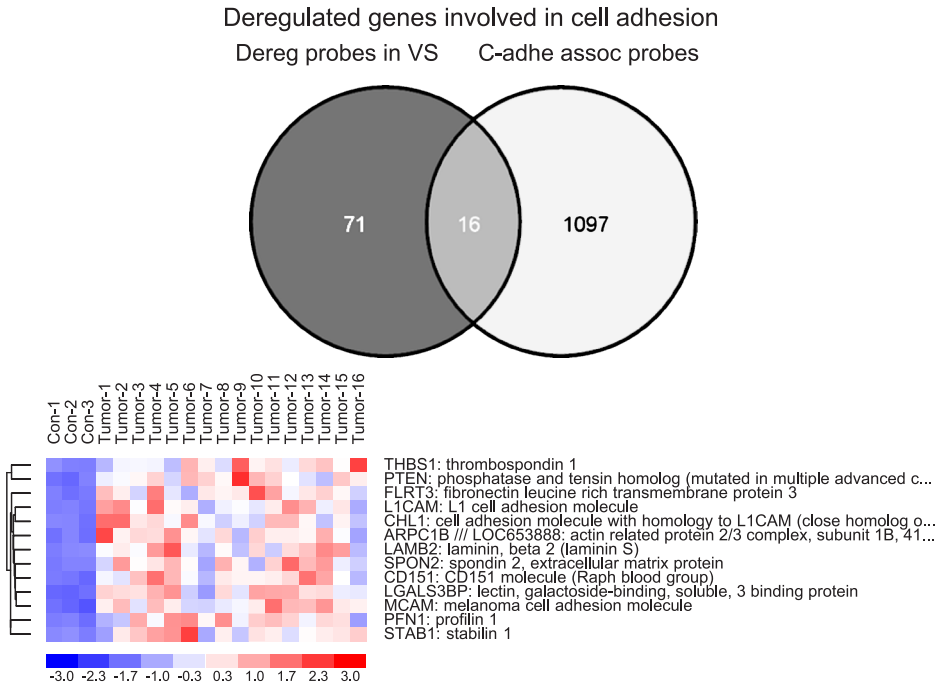

FIG. 7. Deregulated genes associated with cell adhesion. The Venn diagram display that 16 probes (13 genes) are common between the clustered 87 probes (78 genes) and the 1113 probes known to be involved in cell adhesion. The 13 genes were all upregulated in tumor tissue and are listed and aligned next to the results on the "heat-map" for the 16 tumors and the 3 controls (adjacent vestibular nerves). The color intensities of the heat-map indicate the degree of deregulation, for which the standard deviation from the mean values are shown at the *bottom*.

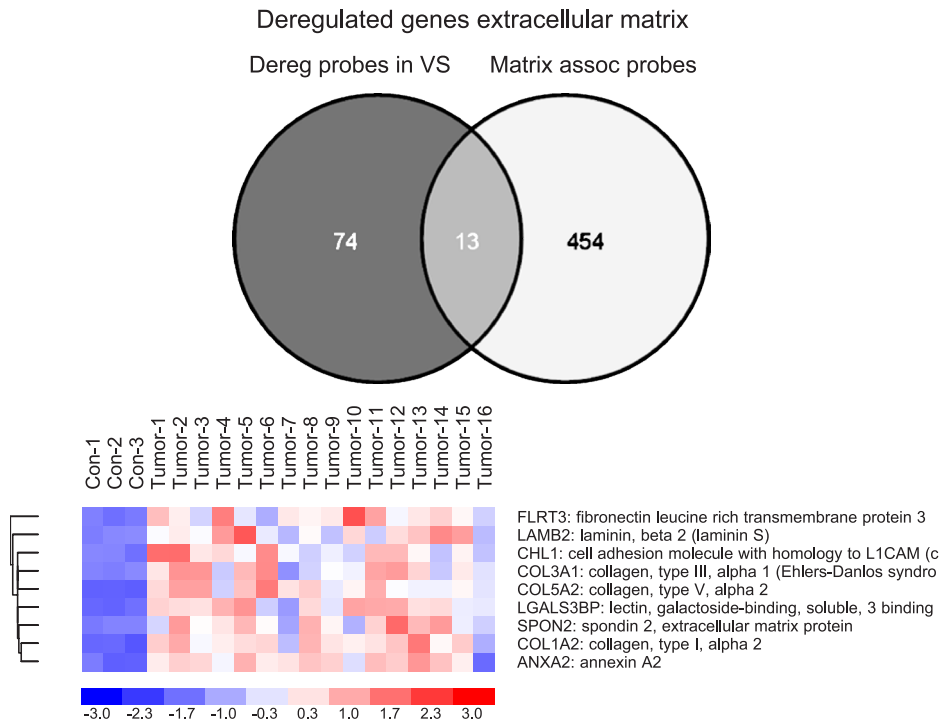

FIG. 8. Deregulated extracellular matrix genes. The Venn diagram display that 13 probes (9 genes) are common between the clustered 87 probes (78 genes) and the 467 probes known to be associated with the extracellular matrix. The 9 genes were all upregulated in tumor tissue and are listed and aligned next to the results on the "heat-map" for the 16 tumors and the 3 controls (adjacent vestibular nerves). The color intensities of the heat-map indicate the degree of deregulation, for which the standard deviation from the mean values are shown at the *bottom*.

and phenotype of the tumors. As indicated in Table 1, a number of transcripts were upregulated more than 5-fold and 13 genes more than 10-fold.

Several transcripts and their encoded proteins have putative functions of potential biologic relevance for vestibular schwannomas. When the factors were matched against established GO, it was found that 8 of the 75 upregulated genes are involved in regulation of the cell cycle, 6 in cell morphogenesis, 8 in cell development, 11 in cell differentiation, 6 in cell death, 13 in cell adhesion, 9 in extracellular matrix, and 50 in protein binding (overlapping occurring; Figs. 2–8).

Additional analyses of the clustered transcripts showed significant enrichment of annotations for the extracellular matrix, cell adhesion, and protein binding. This is intriguing because mosaic *NF2* (merlin) mutants exhibit a global defect in tissue fusion characterized by ectopic detachment and increased detachment-induced apoptosis in the transgenic study of neuroprogenitors by McLaughlin et al. (9). This indicates that regulation of *NF2* expression is a means of controlling cellular adhesion between Schwann cells, and between Schwann cells and axons within the vestibular nerve, which is in agreement with merlin-associated CD44 implication in cell-cell adhesion, cell-matrix adhesion, and tumor progression (10,11), as well as the fact that merlin colocalizes and interacts with adherence components in confluent cells (12). Furthermore, fibroblasts lacking *NF2* function do not undergo contact-dependent growth inhibition and cannot form stable cadherin-containing cell/cell junctions, which shows that merlin functions as a tumor suppressor by controlling cadherin-mediated cell/cell contact (12). It has also been suggested that merlin mediates contact inhibition of cell growth through signals from the extracellular matrix (13). Thus, the enrichment of gene annotations for the extracellular matrix, cell adhesion, and protein binding in tumor tissue may be an indication of upregulation in response to effects of downregulated or dysfunctional merlin. Accordingly, these functional areas may be important for the development of a vestibular schwannoma and constitute obvious fields of future research.

We found no deregulation of the merlin/schwannomin gene (downregulation expected), again given the previously described conservative criteria. We did, however, find an upregulation of the 4.1-band ezrin-radixin-moesin (FERM) domain (containing 4A; 6.7-fold) and of erythrocyte membrane protein band 4.1 (13-fold). Merlin/schwannomin is very similar to the protein 4.1 superfamily members (including ezrin-radixin-moesin and erythrocyte membrane protein band 4.1) linking the molecules to functions related to the cell membrane and cytoskeleton. The FERM domain is an N-terminal globular domain that occurs in all members of the family and has been suggested to contain key functional domains for merlin.

Radixin and moesin was upregulated, whereas ezrin was downregulated in the study by Welling et al. (6). As the

protein 4.1 superfamily members, RhoB is also involved in organizing the cytoskeleton, and both studies showed an upregulation of RhoB GTPase (activating protein 15; Table 1). Thus, factors with functional relation to merlin/schwannomin seem to be potentially involved in tumor development.

When addressing potential merlin deregulation, it is important to note that the adjacent vestibular nerve control tissue could have a single merlin mutation or loss of heterozygosity, which may explain the lack of a finding of downregulated merlin in tumor tissue. In addition, the protein product may be nonfunctional or dysfunctional in tumor tissue, although transcription and translation are normal, as also previously addressed in general terms.

Apart from the enriched annotations, a number of specific genes are relevant candidates for further research (Table 1). A complete account of the functions of these genes would be too exhaustive for the scope of this article. However, 1 example is platelet-derived growth factor D, which apart from being a growth factor is involved in the cell cycle (Fig. 2) and upregulated more than 54-fold in tumor tissue. Platelet-derived growth factor D is active in the development of the brain and plays a role in glioblastomas/medulloblastomas, as well as other types of cancer (14). Conceivably, growth factors will be involved during growth of the tumor after the initial cellular events leading to its formation and apart from platelet-derived growth factor D, a number of other growth factors or growth factor-associated genes were upregulated in tumor tissue: growth factor receptor-bound protein 14, insulin-like growth factor binding protein 4, and transforming growth factor–β receptor II (Table 1). Transforming growth factor–β plays an essential role in Schwann cell proliferation and differentiation, and is involved in neurotrophic effects of several neurotrophic substances. The expression of the growth factor and its receptors I and II in vestibular schwannomas has been evidenced by immunohistochemistry and RT-PCR (15).

Another interesting upregulated gene is *PTEN* (phosphatase and tensin homolog deleted on chromosome 10), which is involved in the cell cycle, in cell development, differentiation, and adhesion, as well as apoptosis (Figs. 2, 4–7). Apart from being involved in the differentiation of gliomas (16), *PTEN* is the major negative regulator of the growth promoting phosphatidylinositol 3-kinase/AKT pathway, which is activated in vestibular schwannomas, possibly due to lack of merlin inhibition (17). Two other genes with potential relation to the PI3K/AKT pathway were also upregulated: inositol 1,4,5-triphosphate receptor type 1 and WD40 repeat protein interacting with phosphoinositides (Table 1). Phosphoinositides has the potential to convert merlin from the closed to the open conformation, which is essential for function (reviewed in 4).

Welling et al. (6) examined vestibular schwannoma gene expression using the same technology as presently employed. They identified 42 genes upregulated more than 3-fold, whereas 8 genes involved in cell growth and signaling were downregulated. When comparing their data to ours, 4 identical or closely associated genes were upregulated in both studies: Rho GTPase activating protein 15, S100 calcium-binding protein A11 (calgizzarin), fibronectin leucine-rich transmembrane protein 3, and actin-related protein 2/3 complex (Table 1).

Another interesting comparison between the studies is related to the upregulation of osteonectin (SPARC) found by Welling et al. SPARC interacts with extracellular matrix proteins (enriched annotation in our study) and acts as a mediator of angiogenesis. Our results showed an upregulation of the scavenger receptor stabilin 1 (12-fold), which mediates targeting for degradation of SPARC (18).

Although equivalent platforms were used, several reasons may explain the limited degree of accordance between the 2 studies such as differences of material and data set analyses (see preceding sentences). Thus, the pioneering study by Welling et al. included a limited number of 7 heterogenic tumor samples (3 sporadic, 3 cystic, and 1 NF2 tumor) and one control (vestibular nerve), which precluded meaningful statistical analyses. We sampled a homogenic material, including 16 sporadic (unilateral, noncystic) tumors and 3 vestibular nerves as control, the latter being the lower limit for statistical analyses. The sampling of more tumors and especially more control tissue will strengthen the validity of future results from our material.

Lasak et al. (Welling and Chang's group) (19) studied the deregulation of the pRb-CDK pathway in 8 vestibular schwannomas (4 sporadic, 3 cystic, and 1 NF2 tumor) using the same chip and 1 vestibular nerve as control. As the only deregulated gene, *CDK2* was underexpressed, which was confirmed by RT-PCR and immunohistochemistry. Conflictingly, our analysis revealed an upregulation of CK2 (mean, 5-fold).

Cyclin D1 is involved in the cell cycle (Fig. 1) and in the pRb-CDK pathway and was found to be upregulated 7-fold in our material (Table 1). Neff et al. found an upregulation in 2 of 8 tumors and a down-regulation in one. Immunohistochemical studies of cyclin D1 expression have also been conflicting, as Neff et al. (20) found no staining in 15 tumors, and Lassaletta et al. (21) recovered a positive staining in 11 of 21 tumors. Thus, cyclin D1 involvement seems controversial.

Neuregulin-epidermal growth factor receptor (Nrg-Erb) signaling contributes to vestibular schwannoma proliferation (22,23) and has accordingly been suggested as a potential target for pharmacotherapy (24). The expression of genes associated with Nrg-Erb signaling has been quantitated by quantitative PCR, which showed an upregulation of neuregulin, epidermal growth factor receptor, and ErbB2 in most sporadic tumors, using vestibular, sciatic, and greater auricular nerve as control (24). None of a number of genes associated with Nrg-Erb signaling was presently deregulated, again given the previously defined analysis criteria.

Only 3 genes were found to be downregulated in tumor tissue: glycoprotein M6A, ribosomal protein S6 kinase, and vitelliform macular dystrophy 2 (bestrophin 1).

Glycoprotein M6A is a neuron-specific membrane glycoprotein of the brain that possesses putative phosphorylation sites for protein kinase C, acting as a nerve growth factor–gated Ca^{++}-channel in neuronal differentiation. (25) Besides regulating neuronal differentiation (25,26), the membrane-bound glycoprotein is a key modulator for neurite outgrowth (27).

Ribosomal protein S6 kinase is a widely expressed serine/threonine kinase that is activated by phosphoinositide-dependent kinase 1, acting as a key regulator for cell transformation induced by tumor promoters/growth factors such as epidermal growth factor (28). As an example, ribosomal protein S6 kinase is involved in regulation of G2-M cell cycle progression by the ERK5-NFκB signaling pathway (29).

Vitelliform macular dystrophy 2 (bestrophin 1) is member of a newly identified family of proteins that can function both as Cl^{-} channels and as regulators of voltage-gated Ca^{++} channels. The proteins are associated with juvenile macular degeneration and interestingly regulated by cell volume (30).

Optimal control tissue for the analysis of gene deregulation in vestibular schwannomas does not exist. The culturing of Schwann cells leads to altered expression profiles in itself (31), which makes a cell culture control questionable. Fresh, normal vestibular nerve is not accessible for ethical reasons, and postmortem sampling would yield unacceptable amounts of degraded mRNA. Vestibular nerve adjacent a vestibular schwannoma (as presently used) or from a patient undergoing vestibular neurectomy due to Ménière's disease is probably not comparable to a normal nerve when addressing issues of molecular biology, although the nerve may seem microscopically normal (see also previously discussed merlin). Furthermore, the vestibular nerve contains numerous axons, whereas Schwann cells dominate a vestibular schwannoma. Thus, different proportions of mRNA expression would be expected from the different proportions of cell types. These inherent biases should be considered when cautiously interpreting our findings, although adjacent vestibular nerve may be the best control available, as indicated by correlated findings on RNA and protein analysis of vestibular nerve (6).

The present material contains a considerable amount of data, which deserve extensive additional analyses. We are currently investigating different pathways and functional subgroups of genes, for example, growth factors and angiogenesis-related genes, which by function are closely associated with the extracellular matrix presently found to be enriched in tumor tissue. In addition, further studies using other methodologies are needed for verification of the observed changes of gene expression seen by cDNA microarray analyses, for example, RT-PCR and protein analyses.

REFERENCES

1. Rouleau GA, Merel P, Lutchman M, et al. Alteration in a new gene encoding a putative membrane–organizing protein causes neurofibromatosis type 2. *Nature* 1993;363:515–21.
2. Trofatter JA, MacCollin MM, Rutter JL, et al. A novel moesin-, ezrin-, radixin-like gene is a candidate for the neurofibromatosis 2 tumor suppressor. *Cell* 1993;75:826.
3. Sainio M, Zhao F, Heiska L. Neurofibromatosis 2 tumor suppressor protein colocalizes with ezrin and CD44 and associates with actin-containing cytoskeleton. *J Cell Sci* 1997;110:2249–60.
4. Neff BA, Welling DB, Akhmametyeva E, Chang LS. The molecular biology of vestibular schwannomas: dissecting the pathogenic process at the molecular level. *Otol Neurotol* 2006;27:197–208.
5. Welling DB, Packer MD, Chang LS. Molecular studies of vestibular schwannomas: a review. *Curr Opin Otolaryngol Head Neck Surg* 2007;15:341–6.
6. Welling DB, Lasak JM, Akhmametyeva E, Ghaheri B, Chang LS. cDNA microarray analysis of vestibular schwannomas. *Otol Neurotol* 2002;23:736–48.
7. Li C, Wong WH. Model-based analysis of oligonucleotide arrays: expression index computation and outlier detection. *Proc Natl Acad Sci U S A* 2001;98:31–6.
8. Ashburner M, Ball CA, Blake JA, et al. Gene Ontology: tool for the unification of biology. The Gene Ontology Consortium. *Nat Genet* 2000;25:25–9.
9. McLaughlin ME, Kruger GM, Slocum KL, et al. The Nf2 tumor suppressor regulates cell-cell adhesion during tissue fusion. *Proc Natl Acad Sci U S A* 2007;104:3261–6.
10. Herrlich P, Morrison H, Sleeman J, et al. CD44 acts both as a growth and invasiveness-promoting molecule and as a tumor-suppressing cofactor. *Ann N Y Acad Sci* 2000;910:106–18.
11. Sherman L, Sleeman J, Herrlich P, et al. Hyaluronate receptors: key players in growth, differentiation, migration, and tumor progression. *Curr Opin Cell Biol* 1994;6:726–33.
12. Lallemand D, Curto M, Saotome I, Giovannini M, McClatchey AI. NF2 deficiency promotes tumorigenesis and metastasis by destabilizing adherens junction. *Genes Dev* 2003;17:1090–100.
13. Morrison H, Sherman LS, Legg J, et al. The NF2 tumor suppressor gene product, merlin, mediates contact inhibition of growth through interactions with CD44. *Genes Dev* 2001;15:968–80.
14. Reigstad LJ, Varhaug JE, Lillehaug JR. Structural and functional specificities of PDGF-C and PDGF-D, the novel members of the platelet-derived growth factors family. *FEBS J* 2005;272:5723–41.
15. Löttrich M, Mawrin C, Chamaon K, Kirches E, Dietzmann K, Freigang B. Expression of transforming growth factor–beta receptor type 1 and type 2 in human sporadic vestibular Schwannoma. *Pathol Res Pract* 2007;203:245–9.
16. Endersby R, Baker SJ. PTEN signaling in brain: neuropathology and tumorigenesis. *Oncogene* 2008;27:5416–30.
17. Jacob A, Lee TX, Neff BA, Miller S, Welling B, Chang LS. Phosphatidylinositol 3-kinase/AKT pathway activation in human vestibular schwannoma. *Otol Neurotol* 2008;29:58–68.
18. Kzhyshkowska J, Gratchev A, Goerdt S. Stabilin-1, a homeostatic scavenger receptor with multiple functions. *J Cell Mol Med* 2006;10:635–49.
19. Lasak JM, Welling DB, Akhmametyeva EM, Salloum M, Chang LS. Retinoblastoma-cyclin–dependent kinase pathway deregulation in vestibular schwannomas. *Laryngoscope* 2002;112:1555–61.
20. Neff BA, Oberstien E, Lorenz M, Chaudhury AR, Welling DB, Chang LS. Cyclin D(1) and D(3) expression in vestibular schwannomas. *Laryngoscope* 2006;116:423–6.
21. Lassaletta L, Patrón M, Del Río L, et al. Cyclin D1 expression and histopathologic features in vestibular schwannomas. *Otol Neurotol* 2007;28:939–41.
22. Hansen MR, Linthicum FH. Expression of neuregulin and activation of erbB receptors in vestibular schwannomas: possible autocrine loop stimulation. *Otol Neurotol* 2004;25:155–9.
23. Hansen MR, Roehm PC, Chatterjee P, Green SH. Constitutive neuregulin-1/ErbB signaling contributes to human vestibular schwannoma proliferation. *Glia* 2006;53:593–600.
24. Doherty JK, Ongkeko W, Crawley B, Andalibi A, Ryan AF. ErbB and Nrg: potential molecular targets for vestibular schwannoma pharmacotherapy. *Otol Neurotol* 2008;29:50–7.
25. Mukobata S, Hibino T, Sugiyama A, et al. M6a acts as a nerve

growth factor-gated Ca(2+) channel in neuronal differentiation. *Biochem Biophys Res Commun* 2002;297:722–8.
26. Michibata H, Okuno T, Konishi N, et al. Inhibition of mouse GPM6A expression leads to decreased differentiation of neurons derived from mouse embryonic stem cells. *Stem Cells Dev* 2008; 17: 641–51.
27. Fernández ME, Cooper B, Flugge G, Frasch AC. The stress-regulated protein M6a is a key modulator for neurite outgrowth and filopodium/spine formation. *Proc Natl Acad Sci U S A* 2005;102: 17196–201.
28. Cho YY, Yao K, Kim HG, et al. Ribosomal S6 kinase 2 is a key regulator in tumor promoter induced cell transformation. *Cancer Res* 2007;67:8104–12.
29. Cude K, Wang Y, Choi HJ, et al. Regulation of the G2-M cell cycle progression by the ERK5-NFkappaB signaling pathway. *J Cell Biol* 2007;177:253–64.
30. Hartzell HC, Qu Z, Yu K, Xiao Q, Chien LT. Molecular physiology of bestrophins: multifunctional membrane proteins linked to best disease and other retinopathies. *Physiol Rev* 2008; 88: 639–72.
31. Lipshutz RJ, Fodor SP, Gingeras TR, Lockhart DJ. High density synthetic oligonucleotide arrays. *Nat Genet* 1999;21:20–4.